Building and Environment 153 (2019) 77–90

Contents lists available at ScienceDirect

Building and Environment

journal homepage: www.elsevier.com/locate/buildenv

Flexible real-time ventilation design in a subway station accommodating the various outdoor PM_{10} air quality from climate change variation

Qian Li[a], Jorge Loy-Benitez[a], SungKu Heo[a], Seungchul Lee[a], Hongbin Liu[a,b], ChangKyoo Yoo[a,*]

[a] Department of Environmental Science and Engineering, College of Engineering, Kyung Hee University, Yongin, 446-701, South Korea
[b] Co-Innovation Center of Efficient Processing and Utilization of Forest Resources, Nanjing Forestry University, Nanjing, 210037, China

ARTICLE INFO

Keywords:
Subway station
Indoor air quality
Outdoor air condition
Flexible real-time control
Multi-objective optimization
Climate change variations

ABSTRACT

Indoor air quality (IAQ) in subway stations are dynamic due to various time-dependent factors, such as subway schedule, passenger load variance in short time scale, and outdoor air quality variation cause from climate change. To remove the indoor pollutants, a conventional mechanical ventilation system is typically utilized in subway stations; however, the working mechanism does not consider the real-time variation of the factors that may cause energy waste or deficiency. Therefore, for a quick response in controlling the time-varying indoor PM_{10} concentration and to design a well-adapted control system for various outdoor air quality (OAQ), a flexible optimal real-time ventilation control strategy was developed. Moreover, the optimal set-points of the PM_{10} concentration in the platform are determined by the multi-objective genetic algorithm (MOGA) at different time intervals to keep a balance of the energy consumption while maintaining healthy levels of IAQ. Experimentally, three cases were then specified and analyzed based on various outdoor PM_{10} health levels (i.e. clean, moderate, and contaminated). The results show that a real-time ventilation system can keep the platform at a healthy IAQ level in all cases. Under clean outdoor air conditions, the controlled system can reduce the energy consumption of the ventilation system by 10.3%. On the other hand, for the contaminated outdoor air condition, the peak value of the platform PM_{10} concentration was reduced by approximately 14 $\mu g/m^3$ and the indoor air level in an underground station was changed from unhealthy to a moderate level.

1. Introduction

Subway transportation is an environment-friendly transport system that has been closely related to public daily activities and public health issue [1]. In megacities such as Seoul of South Korea, there were approximately 2.86 million people commuted through a subway system on a daily basis within 2016 [2]. Furthermore, due to the high passenger's flow and high capacity of underground subway systems, the ground-level traffic congestion has been reduced by a large extent [3,4]. At the same time, however, the overcrowding and the high frequency of usage leads to the fact that the indoor air quality (IAQ) of the subway system has a great impact on the health of the passengers. There are several pathogenic air pollutants found in subway platform that may cause respiratory symptoms and lung malfunction [5], such as volatile organic compounds (VOC), heavy metals, and particulate matter (PM). Thus, the precise control of indoor air pollutant concentration and the rational regulation of IAQ have been public health concerns [6–10].

In recent years, PM attracted public and researcher's attention due to its potential toxicity and ability of pathogenic factors transmitting. The airborne particulates are designated as Group I carcinogen by International Agency for Research on Cancer (IARC) [11]. In fact, no matter short-term or long-term exposure of the relatively high PM concentration, people may suffer from the particle-related diseases [12]. Megido et al. [13] assessed the toxicity of PM with an aerodynamic diameter less than 10 μm (PM_{10}) and found that 40.2% of total studied particles would be deposited in respiratory tract through inhalation. Many previous studies measured the PM concentration of different subway station worldwide [14–18]. Generally, the PM concentration inside the underground subway station is higher than in open-air condition [19]. Therefore, the control of the PM concentration in subway stations at a health level is essential and necessary for public health. Based on the confined space of the underground subway system, the emission sources of PM can be grouped into two classes, 1) those generated by the ambient that enters the platform, and 2) the others generated inside a subway station. According to some previous research, the major sources of the platform PM_{10} generated inside subway station are the break-related source from the wear of the wheels and

* Corresponding author.
E-mail address: ckyoo@khu.ac.kr (C. Yoo).

https://doi.org/10.1016/j.buildenv.2019.02.029
Received 27 December 2018; Received in revised form 14 February 2019; Accepted 20 February 2019
Available online 27 February 2019
0360-1323/

Nomenclature

BP	Breakpoint
CAI	Comprehensive air-quality index
CIAI	Comprehensive indoor air-quality index
CPI	Control performance index
FB	Feedback controller
FF	Feedforward controllers
FOPTD	First order plus time delay
GHG	Greenhouse gas
HI	Upper bound
I	Index of breakpoint
IAQ	Indoor air quality
IMC	Internal model control tuning methods
ITAE	Integral of the time absolute value of the error
LO	Lower bound
MOGA	Multi-objective genetic algorithm
NSGA-II	Non-dominated sorting genetic algorithm
OAQ	Outdoor air quality
OPM_{10}	PM_{10} from outdoor atmosphere
PEM	Prediction-error minimization
PI	Proportional-integral
PM	Particulate matter
PPM_{10}	PM_{10} in the subway platform
RCS	Real-time control strategy
RPM	Ventilation fan speed
RTO	Real-time optimization
TMS	Telemonitoring system
VOC	Volatile organic compounds
ZN	Ziegler-Nichols tuning method

rails (59.5%) and a small fraction from electric cables abrasion (8.1%). The sources of PM introduced from the outside atmosphere are mainly oil combustion (17%), secondary aerosols (10%), and also soil dust (5.4%) through passengers activity spread and mixed inside the subway station [20–22].

To reduce the PM inside the subway station, ventilation systems are generally used to feed the indoor space with fresh air from the outside for supporting favorable IAQ [23,24]. Moreno et al. [25] estimated the effects of tunnel ventilation condition and station construction on subway platform air quality and found that the overall PM concentrations were reduced with switching on the ventilation system. A new IAQ ventilation control system was introduced by Kim et al. [3] to maintain the PM_{10} concentration at a health level by optimizing the feeding volume of outdoor fresh air. Son et al. [26] assessed magnetic filters on removing PM from the subway tunnel, demonstrating the PM removal efficiency increases with an increasing fan frequency. Without a doubt, the increasing fan frequency corresponds to absolutely the large energy demand [27]. Reducing energy consumption and minimizing the indoor air pollutants are two conflicting requirements for developing an optimal ventilation performance in underground subway systems [28]. As the ventilation fan speed increases, a high flow rate of fresh air from outside enters the subway station to dilute the indoor air pollutant. For this reason, this process results in an energy demand increasing from the ventilation system. On the contrary, when the ventilation fan speed decreases, the IAQ is deteriorated due to the lack of fresh air. This trade-off between energy demand of the ventilation systems and IAQ could be solved by a smart controlling optimization strategy. Many studies have been conducted using different aspects of ventilation optimization with an emphasis on the interdependence of IAQ and energy efficiency. Lee et al. [29] proposed a gain-scheduled ventilation control system, the results showed a reduction in the ventilation system energy consumption by 4% through following a rush hours' time trend-trend. Therefore, the ventilation system is crucial in maintaining the IAQ in the subway station at a health level, and an energy-efficient ventilation control strategy by optimizing the fan frequency is necessary to be investigated.

There is another challenge of developing an energy-efficient ventilation system, which is considering the actual situation of the diurnal pattern of PM_{10} air quality in the subway station. Ventilation systems are required to accommodate the real option of varying conditions to cope with the current and future uncertainty, which is also called real-time control. A real-time control strategy (RCS) is a model-based control scheme with real-time optimization (RTO) techniques to obtain a group of set-points in response to a process occurrence. RCS provides a general concept for monitoring, modeling, design, and testing a control system [30,31]. Besides, RCS is outperformed at the intelligent control that adapts to uncertain and unstructured operating environments [32,33], making it suitable for controlling the IAQ in a subway station. Consequently, RCS has been implemented in various research fields to manage systems that require an immediate response. Wang et al. [34] implemented a real-time control scheme to identify a critical zone and supply an optimal outdoor air demand for minimizing the energy demand of a CO_2-based adaptive demand-controlled ventilation system. Gopal et al. [31] applied RTO to an industrial fermentation process to optimize the set-points according to the current operation. Wang et al. [35] applied an RCS to a complex building with the chilled water system, the operational performance, and energy efficiency significant enhanced by online updating of the model parameters. This method automatically updates the set-points for enhancing the robustness of the control system. RTO techniques are well suited to control a multivariable constrained process and can be easily incorporated into computer control systems. The time-varying factors which disturb the air quality in subway platform are varied, such as subway schedule, passenger load which is in short time scale [36,37] and the outdoor PM_{10} air quality which may be influenced by long term climate change. Furthermore, the outdoor PM_{10} concentration highly depended on the meteorological condition, such as temperature, precipitation, air circulation, which may be frequently disturbed by climate change. Meanwhile, the extreme weather-climate events are also the main factor to cause a large variance of PM_{10} concentration. Therefore, the RCS is implemented to act on the real option of time-varying ventilation loads and the performance of the proposed ventilation system under various outdoor PM_{10} air quality should be analyzed.

In this study, for maintaining the health IAQ level and enhance the energy efficiency of the ventilation system in an underground subway station under real-time OAQ variation, the RCS of the ventilation system is modeled and analyzed. For this aim, an RCS of the underground subway ventilation system is developed by manipulating the ventilation fan speed. At first, an IAQ model of the underground subway station is developed with first order plus time delay (FOPTD) model. Secondly, a proportional-integral (PI) controller and feedforward controllers (FF) are implemented in a ventilation control system to manage the IAQ based on the developed IAQ model. Finally, an RCS is implemented by automatically updating the optimal set-points of the control system determined by MOGA with ventilation energy consumption and average PM_{10} concentration in the platform as the objective function. The flexibility of the proposed real-time ventilation control system is estimated under various OAQ conditions, include 'clean', 'moderate', and 'contaminated'. The energy consumption of controlled ventilation is calculated according to the fan inverter frequency. Meanwhile, the energy consumption of the ventilation system is converted to the corresponding greenhouse gas (GHG) emission to reveal the climate change effect. To estimate the health effect of IAQ to the passenger under the proposed control process, a comprehensive indoor air-quality index (CIAI) in the subway platform is carried out for three outdoor conditions.

2. Materials and methods

2.1. Description of the IAQ system at the D-subway station

This study was carried out at the D-subway station, which is located at line No. 3 in Seoul. As shown in Fig. 1(a), the D-subway station is a three floors underground public infrastructure with two waiting rooms and a platform. There are two ventilation systems inside the subway station to remove indoor air pollutants and keep the IAQ at a healthy level. The ventilation fans import fresh air into the platform (3rd floor of the basement) and waiting rooms (2nd floor of the basement) and the air flows through the staircase exits of each floor to the upper floor. The subway platform is the analysis area of this study with the single entrance of fresh air (ventilation opening) and single way out (stairway). The properties of the ventilation system in the subway platform are shown in Table S1.

The PM_{10} in a subway platform (denoted as PPM_{10}) is selected as the target pollutant to implement the control process. Hourly IAQ data in D-subway station are measured from November 21st to 25th, including PPM_{10} concentration, PM_{10} concentration from nearby outside atmosphere (denoted as OPM_{10}), ventilation fan speed (denoted as RPM), subway schedule, and the number of passengers passing the platform (denoted as passenger). A telemonitoring system (TMS) (Fig. 1(b)) installed in the platform is used to collect the real-time monitoring data (PPM_{10} concentration) and the OPM_{10} concentration is measured at a scavenge port outside the D-subway station. Fig. 2 exhibits the measured real-time data sampled in an hourly resolution. The measured OPM_{10} concentration in Fig. 2(a) shows an unspecified trend compared to other measurements each day, with a relatively high concentration at Day-2 and Day-5. The rush hours describe the crowding in public transport due to the commuting of work. Generally, rush hours occur twice every weekday in the morning (7 a.m.–11 a.m.) and the evening (4 p.m.–8 p.m.). This phenomenon can be clearly shown in the plot of the number of passengers passed the station (shown in Fig. 2(b)). The subway schedule in a weekday follows the same frequency; moreover, the one day pattern is shown in Fig. 2(c). In order to satisfy the commuter volume, subway schedule also presenting two peaks at the rush hours. The manual RPM in weekday have the same pattern which is shown in Fig. 2(d). The RPM is set at its highest capacity (60 Hz) from 6 p.m. to 9 p.m. to handle the pollutants in platform due to overcrowding and high use during these hours. The RPM is then dropped to 40 Hz at 10 p.m. to 12 a.m., and 45 Hz for the other periods of the day. The PPM_{10} concentration has a diurnal variation with two peaks during the rush hours, as shown in Fig. 2(e).

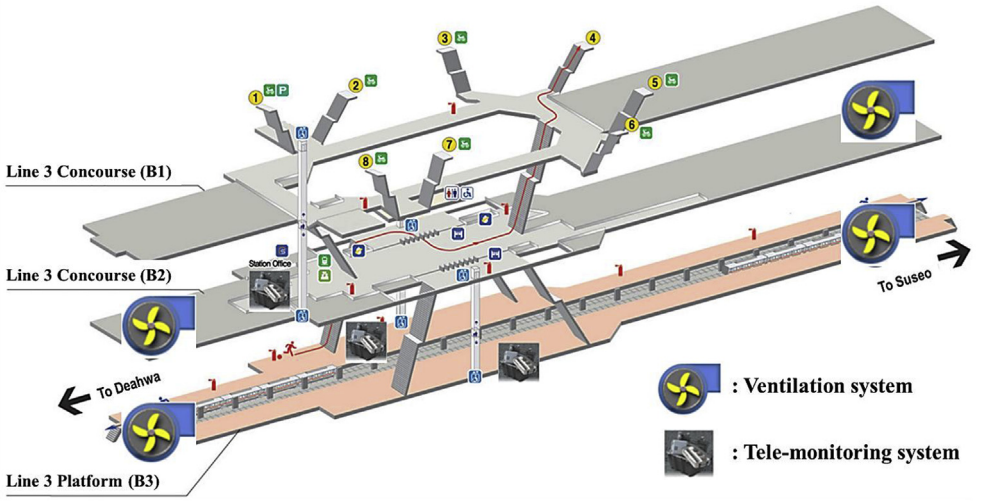

(a)

(b)

Fig. 1. (A) Sketch of the D-subway station and the location of the installed ventilation system. (b) Tele-monitoring system for the IAQ measurements.

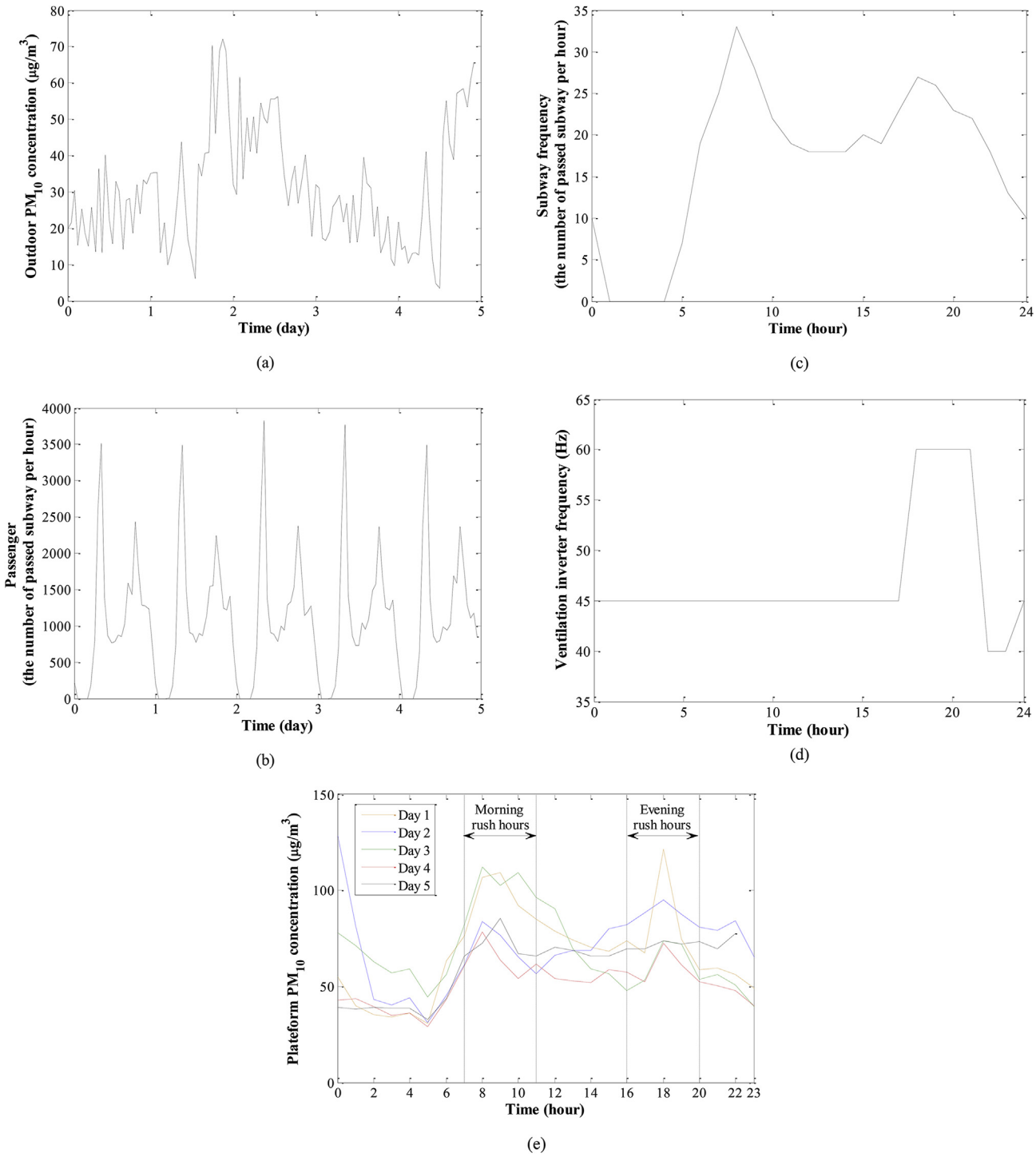

Fig. 2. Variation of IAQ measurement variables from the D-subway station: (a) PM_{10} concentration from outside; (b) passenger number; (c) subway schedule; (d) ventilation inverter frequency; (e) PM_{10} concentration at the station platform.

2.2. Development of the real-time ventilation control system for varying ventilation load

2.2.1. Identification of the IAQ system in the subway platform

Fig. 3 shows the model of the IAQ system that analyzes the relationship among all variables, including subway schedule, passenger, OPM_{10}, and RPM, with the PPM_{10}. The established mathematical model was implemented to predict the PPM_{10} concentration and was used for the ventilation control system. To control the PPM_{10} at a healthy level, the variables which can influence the concentration of PPM_{10} should be specified first. In this research, the PPM_{10} concentration can be affected by manipulated variable (RPM) and three disturbance variables (subway schedule, number of passengers, and OPM_{10} concentrations). Due to the easy implementation and the suitability on describing the dynamic characteristics of a target process, the FOPTD process model is used to identify the IAQ system. The FOPTD process is defined by Eq. (S1) in Supplementary Information (SI) [38].

2.2.2. Ventilation control system

The ventilation control system is modeled to adjust the PPM_{10} by

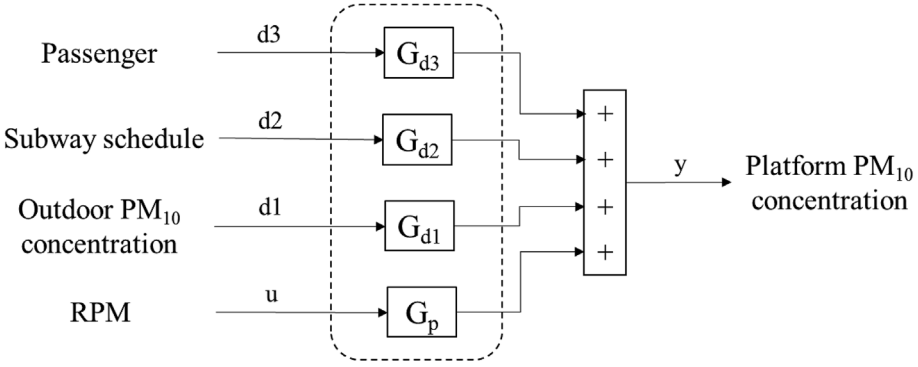

Fig. 3. Schematic diagram of the IAQ ventilation system installed in the D-subway system.

manipulating the RPM. As shown in Fig. 4, the control system integrates a FB controller with three FF (including FF1, FF2, and FF3) controllers. A FB controller is implemented to modulate the signal of PPM_{10} for continuously minimizing the difference (i.e., error value) between the measured value and the desired value (usually called set-point) of the controlled variable. Proportional-integral (PI) controller is a widely used control loop feedback mechanism due to their advantage of simplicity, clear functionality, easy implementation, and high accuracy [38]. To tune the PI controller parameters, Ziegler-Nichols (ZN), internal model control (IMC), and the integral of the time absolute value of the error (ITAE) tuning methods are used and compared. Table S2 gives the expression of tuning rules and their corresponding tuning parameters of a FOPTD model for the PI controller. To compensate the disturbances, three feed-forward controllers (FF1, FF2, and FF3) are implemented to compensate for disturbances of OPM_{10}, subway schedule, and passengers on the PPM_{10} concentration by regulating the RPM. Theoretically, FF controllers can eliminate the effects of disturbances, and the control performance can be further improved by combining FB and FF controllers. The detail information of FB and FF controller are shown in SI.

The best ventilation control configuration should be determined before implementing the RCS, which can both save the energy from the ventilation system and improve the air quality in the platform. According to the aim of this study, the optimal strategy needs to be found which can success minimizing the PPM_{10} concentration within the health region and efficiently reduce energy consumption from the ventilation system at the same time. Therefore, a control performance index (CPI) is introduced for the proposed ventilation control system using Eq. (1).

$$CPI = C_{\text{platform}} + E_{\text{ventilation}} \tag{1}$$

where C_{platform} is the average concentration of PPM_{10} during an operation day, and $E_{\text{ventilation}}$ is the average ventilation energy demand during an operation day. The C_{platform} can be calculated from the ventilation model (shown in section 2.2.2). To simplify the calculation of the ventilation energy consumption, the ambient conditions (such as ambient temperature and humidity) were not considered. Then, the $E_{\text{ventilation}}$ can be expressed as a third order polynomial regression model using RPM [7]:

$$E_{\text{ventilation}} = 0.0007 \times RPM^3 - 0.046 \times RPM^2 + 2.01 \times RPM + 8.8 \tag{2}$$

For the purpose of designing an energy-efficiency ventilation control system meanwhile maintaining the healthy IAQ level inside the subway platform, the IAQ level and energy consumption which reflected by CPI should be minimized. Therefore, a controlling system with the lowest value of CPI is expected.

2.2.3. Real-time control strategy

In the subway platform, the complex IAQ process shows a temporal pattern caused by many disturbances, which can be adjusted into a healthy range by installing a ventilation system. However, the RPM in the conventional ventilation system is a little bit stubborn and cannot provide a good response to the ventilation system to time-varying disturbance loads. On the contrary, the intelligent ventilation system can give an immediate response to the changes of disturbances and, therefore, the control process is dynamically updating set-point of the ventilation control system to achieve the goal of maintaining IAQ at health level with the minimal energy consumption.

A general RCS is composed of four parts, which followed the order of monitoring, prediction, optimization, and control [31,36]. To

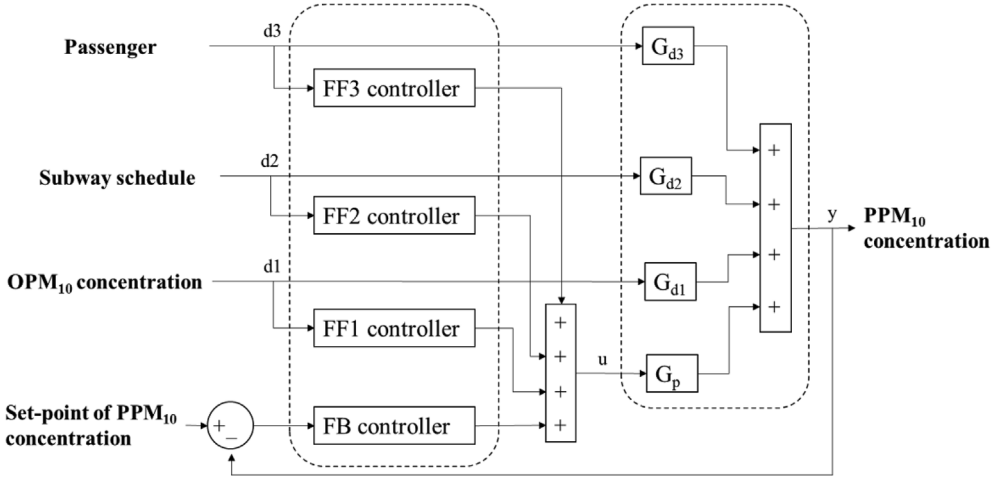

Fig. 4. Block diagram of the ventilation control system.

implement the RCS, the operational data should be measured and monitored at first. Then, the system condition is predicted in a predefined time range. Based on the predicted system condition, the set-points of the control process are estimated by optimizing an objective function. Finally, the optimal set-point at each time period is implemented into the control process, which contributes to the increase of control efficiency.

As shown in Fig. 5, the proposed schematic diagram of the RCS of ventilation system considering real options consists of three parts: (1) development of the IAQ prediction model, (2) ventilation control system design, and (3) implementation of the RCS to the ventilation control system. Hourly IAQ data is continuously collected by the TMS, and then the IAQ prediction model is developed by four FOPTD models. Three FF and one FB controllers are then integrated for constructing the ventilation control system. Based on the developed ventilation control system, RCS is applied to determine the best way to operate the ventilation system in the subway platform. In this context, 'best' means maintaining the healthy IAQ in the subway platform while saving energy. The optimal solution is achieved by selecting an appropriate group of set-points for the PPM_{10}. The set-points, which are evaluated by a MOGA and updated per specific time interval, are fed to the ventilation control system to give the response of the real-time disturbance variance.

2.2.4. Multi-objective genetic algorithm for set-point optimization

MOGA is an advanced optimization method for solving complex optimization problems based on the natural selection principle. A series of local Pareto fronts for multiple objective functions are searched by using the genetic algorithm. To search for a reasonable Pareto set, the non-dominated sorting genetic algorithm (NSGA-II) is the most widely implemented method [28,39]. MOGA is carried out in this research to determine the proper optimal set-points of RCS in the subway platform ventilation system to realize the two objectives. The first objective is to minimize the PPM_{10}, and the second is to minimize the energy consumption from the ventilation system.

2.3. The proposed method

As shown in Fig. 6, the proposed schematic diagram of the real-time ventilation control strategy consists of five stages: (1) data collection and preprocessing, (2) developing the IAQ prediction model, (3) designing the ventilation control system and estimating the control performance, (4) developing real-time ventilation control system, and (5) implementation of the real-time control strategy under various OPM_{10} conditions and evaluate the passengers' health risk.

Firstly, with the IAQ variables previously collected, the prediction model for the PPM_{10} concentration is constructed by four FOPTD models of the RPM, OPM_{10}, subway schedules, and passenger, which is identified by the prediction-error minimization (PEM) method. Secondly, three FF and one FB controllers are designed for constructing the ventilation control system. In this part, three tuning methods, ZN, IMC, and ITAE, are performed to tune the parameters of the PI controller. Then, the real-time ventilation control system is implemented by updating the set-points of the ventilation control system at several time intervals (2, 3, 4, 6, 8, 12 and 24 h) to minimize both the energy demand of the ventilation system and the PPM_{10} concentration. Finally, to evaluate the control performance of the proposed method, the average value of the PM_{10} concentration at the platform and the energy demand of the ventilation system are used as performance criteria. The proposed method is implemented under three OPM_{10} conditions ('clean', 'moderate', and 'contaminated') and compared with manual control (with conventional RPM).

2.4. OPM_{10} conditions determined by comprehensive air-quality index

The different OPM_{10} conditions are specified by the comprehensive air-quality index (CAI) proposed by the Korean Ministry of Environmental [40], which is a guideline for figuring out the health risk level of ambient air pollution. CAI aims to give the public an easy way to understand outdoor air condition and protect themselves from contaminated air. Table S3 shows the CAI category, which is divided into four levels, good, moderate, unhealthy, and very unhealthy. According to the CAI, the PM_{10} at the 'good' level corresponds to an upper concentration threshold of 30 $\mu g/m^3$ and the PM_{10} at the 'moderate' level is

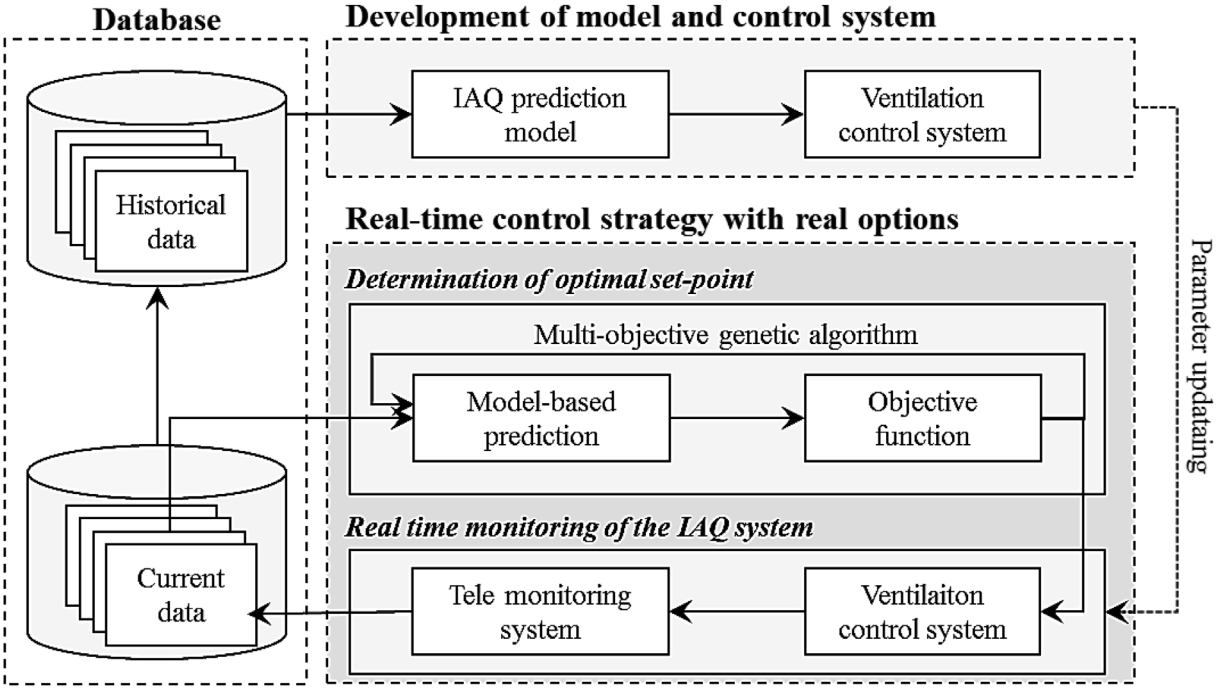

Fig. 5. The schematic diagram of the proposed real-time ventilation control strategy under real options of varying ventilation load.

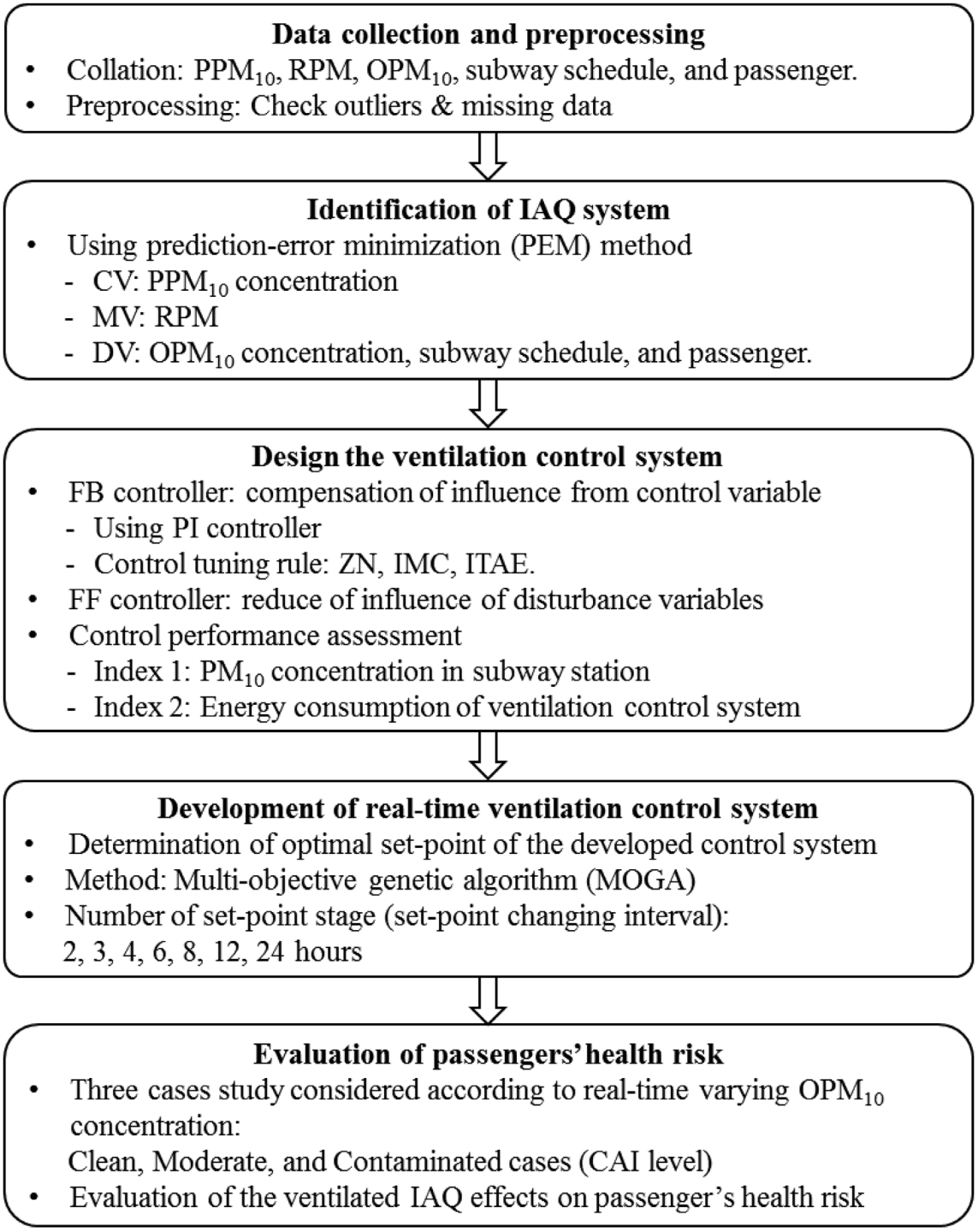

Fig. 6. The procedure of the proposed real-time ventilation control strategy.

the concentration greater than 31 and less than 80 μg/m^3 'Unhealthy' level PM_{10} exceeds 81 μg/m^3 [41]. Three OPM_{10} conditions are specified based on CAI and three case studies are donated as clean, moderate, and contaminated corresponding to the OPM_{10} under the CAI of 'good', 'moderate', and 'unhealthy', respectively. Fig. 7(a) shows the hourly variation of the OPM_{10} concentrations (clean: July 11th to July 15th; moderate: Nov. 21st to Nov. 25th; contaminated: Jan 31st to Feb 4th). Basic statistics measurements are presented as boxplots shown in Fig. 7(b). The average OPM_{10} concentration for these three cases is 12.28 μg/m^3, 31.51 μg/m^3, and 103.04 μg/m^3 for clean, moderate, and contaminated case, respectively. In the clean case, almost all the samples belong to the 'good' level of health concern suggested by CAI. In the moderate case, half of the data belongs to the 'moderate' level. For the contaminated case, 58% of the samples belong to the 'unhealthy' level.

3. Results and discussion

3.1. IAQ system modeling in D-subway station

Four FOPTD models are performed in the IAQ ventilation system to predict the PPM_{10}. The process model from a manipulated variable

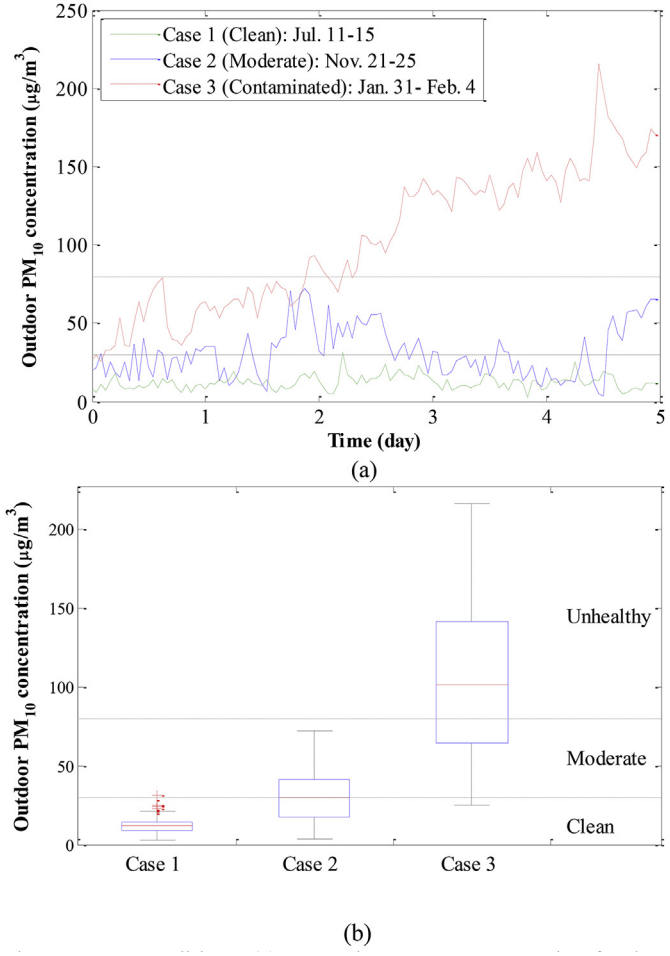

Fig. 7. Various OPM_{10} conditions. (a) Dynamic OPM_{10} concentration for three cases: clean, moderate, and contaminated. (b) Boxplot of the three OPM_{10} concentrations.

Table 1
Tuning parameters of the PI controller in IAQ ventilation system.

Tuning rule	Proportional gain	Integral gain
ZN	−0.548	-1.25×10^{-6}
IMC	−0.382	0.0347
ITAE-1	−0.0357	−0.00076

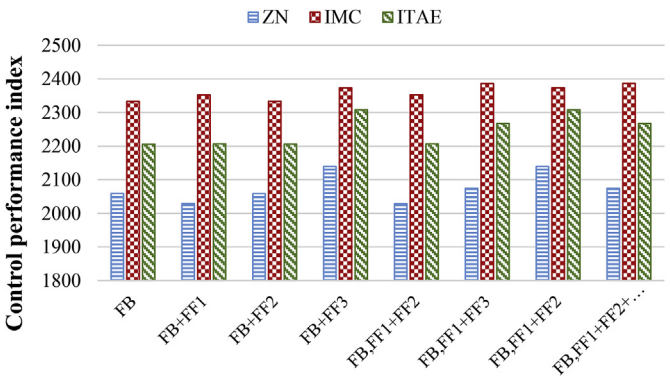

Fig. 8. Control performance index under various control configurations with ZN, IMC, and ITAE to tune the parameters in the PI controller.

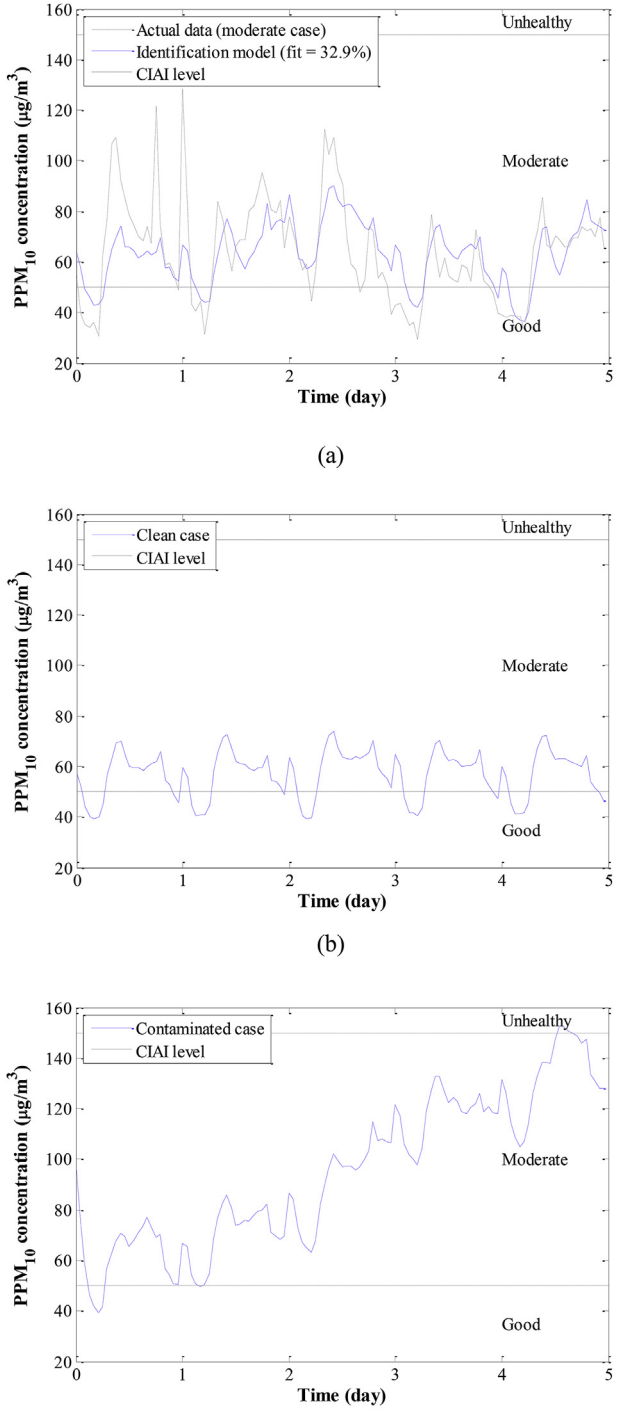

Fig. 9. Simulation results of the predicted PPM_{10} concentration using the IAQ ventilation model under (a) moderate, (b) clean, and (c) contaminated outdoor conditions.

(RPM) to the controlled variable (PPM_{10}) is present as follows:

$$G_p(s) = \frac{-0.829s}{0.00248s + 1} \exp(-0.0644s) \tag{3}$$

The negative sign of the process gain in Eq. (3) indicates that the PPM_{10} concentration decreases 0.829 times when the RPM signal increases per unit. The time delay in this process is 0.0644, representing that it needs approximately 92 min for the RPM to adjust the PPM_{10} concentration to meet the target concentration. Furthermore, the time

Table 2
Comparison of the average PPM_{10} concentration and energy demand of the ventilation system with respect to the manual control and real-time control set point optimization under the clean outdoor condition.

Control configuration	Time interval for updating set-point (hour)	PM_{10} concentration ($\mu g/m^3$)	Energy consumption (kWh/day)	Average RPM (Hz)
Conventional	/	56.99	1838.78	47.1
RCS	24	60.07	1637.52	43.5
	12	57.46	1803.35	46.7
	8	57.38	1803.42	46.8
	6	57.38	1801.77	46.7
	4	58.08	1755.97	45.8
	3	57.97	1761.96	46.0
	2	57.95	1773.02	46.1

Table 3
Comparison of the average PPM_{10} concentration and energy demand of the ventilation system with respect to the manual control and real-time control set point optimization under the moderate outdoor condition.

Control configuration	Time interval for updating set-point (hour)	PM_{10} concentration ($\mu g/m^3$)	Energy consumption (kWh/day)	Average RPM (Hz)
Conventional	/	64.01	1838.78	47.1
RCS	24	63.68	1889.87	46.8
	12	64.59	1832.23	45.7
	8	64.47	1837.68	45.9
	6	64.66	1826.27	45.6
	4	64.69	1828.34	45.6
	3	64.76	1822.01	45.5
	2	64.70	1828.42	45.6

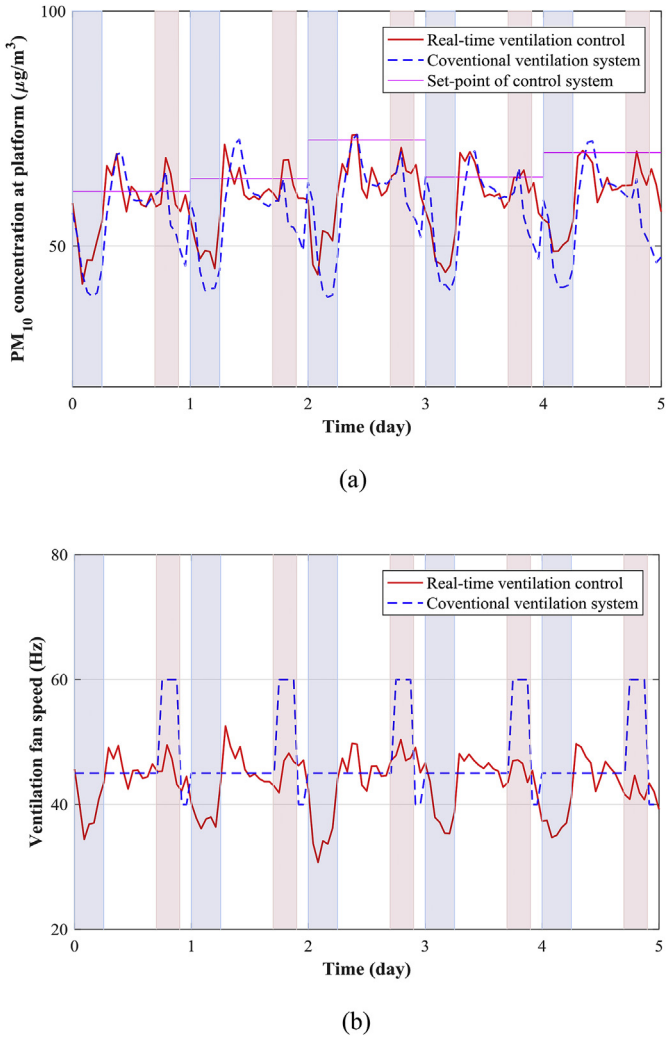

Fig. 10. Control performance of real-time ventilation control by updating set-points every 24 h under a clean outdoor condition. (a) The controlled PM_{10} concentration at the platform and (b) ventilation fan speed.

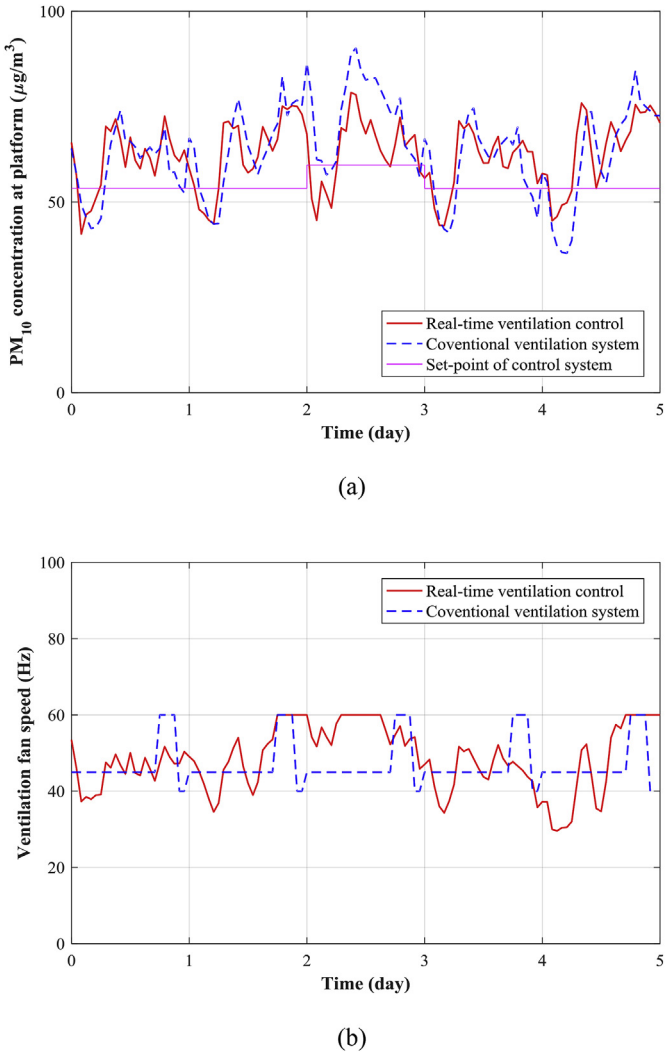

Fig. 11. Control performance of real-time ventilation control with updated set-points every 24 h under a moderate outdoor condition. (a) The controlled PM_{10} concentration at the platform and (b) ventilation fan speed.

constant was 0.00248, indicating that the PPM_{10} concentration gradually changes and it takes 3.57 min to reach the 63% of the total variation of the PPM_{10} variation.

The FOPTD models, used for illustrating the relation between three disturbance variables, including OPM_{10} (d1), subway schedule (d2), and passenger (d3), are shown in Eqs. (4)–(6).

$$G_{d1}(s) = \frac{0.674s}{0.110s + 1} \tag{4}$$

$$G_{d2}(s) = \frac{0.000421s}{0.9901s + 1}\exp(-0.1s) \tag{5}$$

$$G_{d3}(s) = \frac{1.012s}{0.0164s + 1}\exp(-0.0275s) \tag{6}$$

Table 4
Comparison of the average PPM_{10} concentration and energy demand of the ventilation system with respect to the manual control and real-time control set point optimization under the contaminated outdoor condition.

Control configuration	Time interval for updating set-point (hour)	PM_{10} concentration ($\mu g/m^3$)	Energy consumption (kWh/day)	Average RPM (Hz)
Conventional	/	94.90	1838.78	47.1
RCS	24	90.81	2288.35	52.4
	12	91.44	2233.84	51.7
	8	91.20	2233.26	51.9
	6	91.45	2212.91	51.6
	4	91.28	2233.62	51.8
	3	91.89	2190.24	51.1
	2	92.54	2158.49	50.3

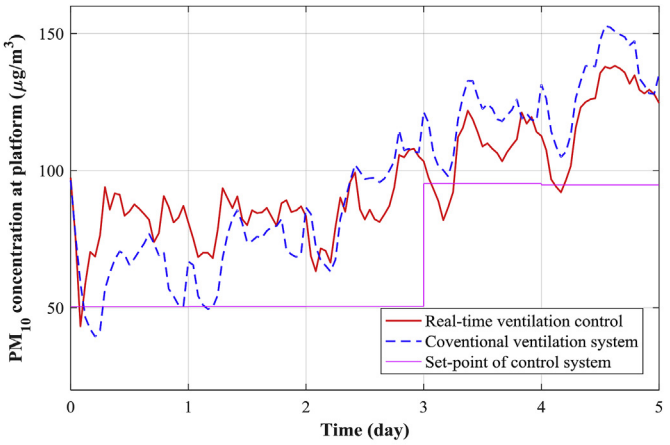

Fig. 12. Control performance of real-time ventilation control with updated set-points every 24 h under a contaminated outdoor condition. (a) Controlled PM_{10} concentration at the platform and (b) ventilation fan speed.

Based on these FOPTD models, the relationship between the disturbance variables is clearly identified. The positive impacts of the three input variables on the PPM_{10} are detected (the process gains of these three FOPTD model are positive). Additionally, the process gain, i.e. numerator in the three transfer functions, shows the magnitude of changes from output variables caused by the input variables. The largest value is shown in Eq. (6) indicating that the passenger has a larger impact on the PPM_{10} than the other two factors (OPM_{10} and subway schedule). The influence factor of the subway passengers contributes to the soil and road dust in the platform. The process gain obtained in Eq. (4) verified the particles introduced from the outdoors are the second source of the PPM_{10}.

3.2. Ventilation control system and tuning parameters

According to the identified IAQ system, the ventilation control system integrated with one FB and three FF controllers is implemented. The FB controller has a PI structure to minimize the difference between the set-point and measured data of PPM_{10} concentration. Three tuning methods (ZN, IMC, and ITAE) are applied to enhance the PI controller parameters, and the tuned parameters are shown in Table 1. The proportional term considers that the magnitude of the measured variables moves away from the desired set-point. The proportional gain calculated by three tuning rules are negative and greater than the minus one, which means that at a fixed interval of time, the proportional term subtracts the error between the process current output and the desired set-point. The integral term addresses how long the measured variables are separated from the desired set-point. If the absolute value of the tuned integral gain is quite large, it can lead to unstable of ventilation control system by causing the fluctuated of fan speed. Therefore, the PI controller with parameter determined using ZN tuning method may result in a more stable ventilation system.

Three FF controllers are implemented for eliminating the effect from the OPM_{10} (G_{FF1}), the subway schedule (G_{FF2}), and the number of passengers (G_{FF3}). The transfer functions of these three FF controllers are shown in Eqs. (7)–(9), respectively:

$$G_{FF1} = \frac{0.00167s + 0.674}{0.0913s + 0.829} \tag{7}$$

$$G_{FF2} = \frac{1 \times 10^{-6}s + 0.000421}{0.822s + 0.829}\exp(-0.356s) \tag{8}$$

$$G_{FF3} = \frac{0.00252s + 1.0186}{0.0136s + 0.829} \tag{9}$$

The control performance of a system is highly dependent on the control configuration. To determine the proper control configuration among the eight suggested control strategies in terms of FB controller and FF controllers, the fixed desired concentration of the PPM_{10} is set to 59 $\mu g/m^3$. The CPI of the IAQ ventilation control system is shown in Fig. 8. According to the CPI, the ZN tuning rule is selected to determine the PI controller parameters. Besides, the combination of FB, FF1, and FF2 controllers are the most appropriate strategy for the objectives of energy conservation and keeping the concentration of the PPM_{10} at a healthy level.

3.3. Optimal real-time ventilation control system under various outdoor air conditions

The proposed real-time ventilation control system is established with an FB (PI controller with ZN tuning rule) and two FF (FF1 and FF2) controllers to minimize the energy consumption of ventilation system and maintain the PM_{10} concentration at the platform at the healthy level (PM_{10} concentration less than 120 $\mu g/m^3$). The set-point of the real-time ventilation control system is updated at various time intervals (2, 3, 4, 6, 8, 12, and 24 h) where each set-point is optimized by the MOGA with 30 individuals (as population size) and 100 generations. Various OPM_{10} concentration conditions (clean, moderate, and contaminated) are analyzed for the proposed real-time ventilation control system.

Fig. 9 shows the simulation results of the PPM_{10} concentration obtained from the IAQ system under three OPM_{10} conditions (clean, moderate, and contaminated). Fig. 9(a) presents the observed and simulated PPM_{10} concentration under moderate outdoor condition. The

Table 5
The improvement of average PPM_{10} concentration and ventilation system energy consumption under three OPM_{10} conditions.

Cases	Control configuration	PPM_{10} concentration		Energy consumption		CO_2 emissions
		Value (μg/m^3)	Improvement factor (%)	Value (kWh/day)	Improvement factor (%)	Value (kg/day)
Clean	Conventional	56.99	5.3%	1826.70	−10.4%	955.18
	RCS-24 h	60.07		1637.52		856.26
Moderate	Conventional	64.01	−0.5%	1826.70	3.5%	955.18
	RCS-24 h	63.68		1889.87		988.21
Contaminated	Conventional	94.90	−4.3%	1826.70	25.3%	955.18
	RCS-24 h	90.81		2288.35		1196.58

predicted PPM_{10} concentration had a reasonable 32.9% fitness with the observed PPM_{10} concentration. And the IAQ system can detect the variation tendency caused by the time-varying influence factor. The established IAQ system is also implemented to estimate the PPM_{10} concentration under clean and contaminated outdoor conditions, which are described in Fig. 9(b) and (c). Under the clean OPM_{10} condition, the PPM_{10} concentration has an apparent trend of periodic change, which means that the subway schedule and passengers may become the main factors influencing the PPM_{10} concentration. Under a contaminated OPM_{10} concentration, the overall tendency of the PPM_{10} concentration is increasing due to the influence of the increasing OPM_{10} concentration. The periodic change of the PPM_{10} concentration can be also observed in the unhealthy condition, where the lowest value exists around 5 a.m. and the peak values appear around 11 a.m. and 6 p.m.

3.3.1. Real-time ventilation control under the clean OPM_{10} condition

Table 2 shows the optimal results of the clean OPM_{10} condition for two control performance values, where the PPM_{10} concentration and ventilation energy consumption are obtained using the MOGA method in the real-time ventilation control system. The average value of the PPM_{10} concentration under the control system is higher than the conventional system during all time interval scenarios. Meanwhile, the energy consumption of the ventilation system is reduced distinctly. More specifically, by updating the set-points every 24 h, the energy consumption is reduced by approximately 10% compared to the conventional system, and meanwhile, the correlated PPM_{10} concentration is increased to 60 μg/m^3, which is still in the healthy level for passenger health. As the outdoor air is clean, there is little influence from outdoor. Thus, the RCS in this case is more focused on reducing the energy consumption of the ventilation system.

Fig. 10 illustrates the control performance of the real-time ventilation control system by updating set-points every 24 h under clean outdoor conditions. As shown in Fig. 10(a), the set-points are greater than the average value of the PPM_{10} concentration which indicates that the ventilation fan speed can keep at a low level due to the good IAQ of the platform. Fig. 10(b) shows the comparisons of ventilation fan speed managing between the conventional system and real-time ventilation control system. Compared with the conventional system, the control ventilation fan speed is lower than the conventional case from 0 a.m. to 6 a.m. (blue shadow), and the corresponding PPM_{10} concentration at this time period is higher. From 6 p.m. to 9 p.m. (red shadow), the controlled ventilation fan speed is also less than the conventional system. Therefore, the real-time ventilation control system under a clean OPM_{10} condition can reduce the energy consumption of the ventilation system, and the PPM_{10} concentration is maintained at a healthy level at the same time.

3.3.2. Real-time ventilation control under the moderate OPM_{10} condition

As shown in Table 3, two values ($PPM_{10,}$ and ventilation energy consumption), which reflect the control performance, are obtained using the MOGA method in the real-time ventilation system under the moderate outdoor condition and the results are. There is no obvious difference between the average values of PPM_{10} concentration under RCS and conventional control strategy. Due to the conflict relationship between the PPM_{10} and energy consumption, the average value of the PPM_{10} decreases as the energy consumption goes up. It therefore follows that the 24-h time interval scenario has the lowest average PPM_{10} and the highest average energy consumption among the RCSs.

Compared with the conventional system, the controlled ventilation fan speed is lower from 0 a.m. to 6 a.m., and the corresponding PM_{10} concentration of the platform at this time period is higher. From 6 p.m. to 9 p.m., the controlled ventilation fan speed is also lower than the conventional system. Therefore, the real-time ventilation control system under a clean OPM_{10} condition can reduce the energy consumption of the ventilation system while keeping a healthy level of PPM_{10} concentration. Fig. 11 explains the control performance of the real-time ventilation control with updated set-points every 24 h under moderate outdoor condition. The PPM_{10} concentration at a high level was reduced (Day 3) and at a low level was increased (2 a.m.–6 a.m. on Day 5). Over the whole period, the PPM_{10} concentration under the RCS becomes more stable than the conventional system. On the third day, the average value of the PPM_{10} concentration is reduced from 68.91 μg/m^3 to 65.56 μg/m^3 and the peak value is reduced by approximately 12 μg/m^3. From Fig. 11(b), the ventilation fan speed is high in the period, form end of Day 2 to end of Day 3, to compensate for the increasing PPM_{10} concentration. This phenomenon is due to the relatively high values of external disturbances in the OPM_{10}.

3.3.3. Real-time ventilation control under the contaminated OPM_{10} condition

Under the contaminated OPM_{10} condition, two control performance values, PPM_{10} concentration, and ventilation energy consumption are summarized in Table 4. Due to the contaminated outdoor condition, the PPM_{10} concentration is higher than those of the aforementioned conditions. According to the table, the RCS shows more contribution to reducing the energy consumption for which the controlled average PPM_{10} concentration is less than the conventional system. Besides, the scenario with a 24-h time interval has the minimum average PPM_{10} concentration.

Fig. 12 shows the control performance of the real-time ventilation control by updating set-points every 24 h under the contaminated outdoor condition. Due to the concentration of PM_{10} outside having a similar increasing trend with the PPM_{10} concentration, the OPM_{10} concentration influences the PPM_{10} concentration more than the other two disturbances (subway schedule and passengers). In Fig. 12(a), the set-points for all time intervals are less than the average PPM_{10} concentration, which aims to reduce the indoor PM_{10} concentration. The set-points for the last three days are greater than the other two days. This phenomenon is due to the relatively high values of external disturbance of outside PM_{10}. Within the last three days, the controlled PPM_{10} concentration is much lower than the conventional system. The peak value on the last day is reduced from 152 μg/m^3 to 138 μg/m^3. According to the ventilation fan speed shown in Fig. 12(b), it is clear that the controlled ventilation increases to the highest level in the last three days.

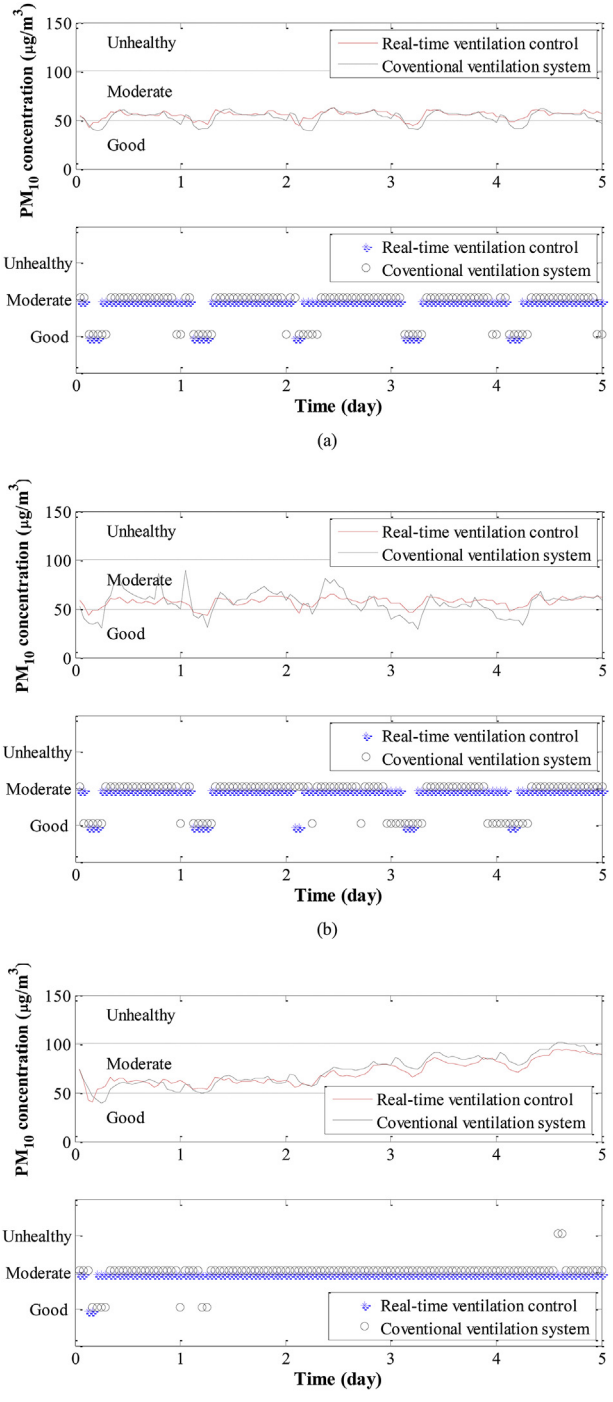

Fig. 13. CIAI level of the PPM_{10} under (a) clean, (b) moderate, and (c) contaminated OPM_{10} conditions in the D-subway station.

3.4. Evaluation of the system flexibility and the passengers' health risk

Table 5 summarizes the managed performance (including average PPM_{10} concentration and the energy consumption of ventilation system) among the RCS (updating set-points every 24 h) and the conventional strategy when dealing with three OPM_{10} conditions (clean, moderated, and contaminated). The real-time ventilation system with updated set-points every 24 h shows good flexibility for all three cases (Tables 2–4). Compared with the conventional strategy, the energy consumption of a controlled ventilation system in the case of clean OPM_{10} condition is reduced by approximately 10.4%, and the PPM_{10} concentration is increased by 5.3%. In the case of moderated OPM_{10} condition, the control system reduced 0.5% average PPM_{10} concentration and the energy consumption is increased by 3.5%. Under the contaminated OPM_{10} condition, the PPM_{10} concentration is reduced for 4.3% and the energy consumption is increased by 25.3%. Obviously, the proposed RCS of the ventilation system is capable of reducing energy consumption when keeping OPM_{10} at a good level. When the OPM_{10} is contaminated, the controlled system contributes to improve air quality. Overall, the proposed RCS of the ventilation system can intelligently control the IAQ inside subway platform.

To estimate the designed ventilation system on climate effect, the energy consumption of the ventilation system can be expressed as the amount of GHG emission per functional unit of electricity consumption. According to related literature, a ratio of 0.5229 kg CO_2/kWh was assumed to calculate the GHG emissions from the ventilation system [42]. The results are shown in Table 5. The conventional ventilation system accounts about 1826.7 kWh for daily operation and the related CO_2 emission is 955.18 kg. In the case of clean outdoor air condition, there is nearly 99 kg CO_2 can be reduced during one day's operation. In the case of moderate and contaminated OPM_{10} conditions, the corresponding GHG emission is 988.21 kg and 1196.58 kg, respectively. It seems that the proposed RCS of the ventilation system cannot contribute to the mitigation of climate change under moderate and contaminated OPM_{10} cases, but the contribution on keeping the IAQ cannot be neglected.

Fig. 13 shows the CIAI level of the PPM_{10} under three OPM_{10} conditions, Fig. 13(a), (b), (c) correspond to clean, moderate, and contaminated outdoor conditions, respectively. For each figure, the upper plot shows the CIAI value of the PPM_{10} concentration and the lower plot shows the healthy level of each data point. As shown in Fig. 13(a), all the PPM_{10} concentrations are at good and moderate levels under the clean outdoor condition in both conventional and controlled cases. Among the most time points, the PPM_{10} can maintain in the moderated level. Comparing the controlled system with the conventional system, there are more PPM_{10} data points that change from 'clean' level to 'moderated' level, which is due to the reduction of ventilation fan speed. Therefore, the energy can be saved from the ventilation system without increasing the PPM_{10} concentration significantly. Fig. 13(b) shows the CIAI level of PPM_{10} under the moderate OPM_{10} condition. Similarly, the PPM_{10} concentrations during the experiment period are at good and moderate levels under the moderate outdoor condition. Meanwhile, the CIAI of controlled PPM_{10} at some time points are changed from good level to moderate level. In the contaminated OPM_{10} condition, most data locate at the moderate level region in the plot of Fig. 13(c). In the conventional system, the PPM_{10} is unhealthy for sensitive people in the last day but the PM_{10} concentration is reduced to a moderate level under the controlled system. Therefore, the proposed real-time ventilation control system can maintain the PPM_{10} at a healthy level under various influences from OPM_{10} and can also save energy for the ventilation system.

4. Conclusion

An RCS of ventilation system was developed in this study to keep the PM_{10} concentration in a subway platform at a healthy range as well as reduce the energy consumption of the ventilation system. Three case studies with different OPM_{10} condition were analyzed and compared in this study for evaluating the climate adaption of the designed ventilation system. The RTO was implemented by using MOGA in the real-time ventilation control system to determine the optimal set-points at each time interval and updating the set-points of the control system to provide quick response to the ventilation fan speed when suffering the time-varying disturbances. The proposed RCS with optimal set points refreshed at 24 h interval shows high flexibility for efficiently operating the ventilation system and maintaining the PPM_{10} concentration under the health level of various OPM_{10} concentrations. The results of this

study show that the designed RCS for manipulating the ventilation system can reduce 10.3% of the energy consumption in comparison with the conventional control strategy under clean OPM_{10} condition. In the moderate OPM_{10} condition, the value of the PPM_{10} was smoother than the conventional system and the peak value on the third day was reduced to 12 $\mu g/m^3$. Under contaminated OPM_{10} condition, the PPM_{10} concentration at a high level was mainly caused by the increasing OPM_{10}, which could be efficiently reduced by the real-time ventilation control system. Thus, the PPM_{10} concentration can be adjusted to healthy level from unhealthy level. Above all, taking the OAQ into account, the real-time ventilation control system can result in the robust ventilation control performance by saving energy and enhancing the IAQ level of subway platforms at the same time under various OAQ condition.

Acknowledgments

This work was supported by a National Research Foundation of Korea grant funded by the Korean government (MSIT) (No.2017R1E1A1A03070713) and Korea Ministry of Environment (MOE) as Graduate School specialized in Climate Change.

Appendix A. Supplementary data

Supplementary data to this article can be found online at https://doi.org/10.1016/j.buildenv.2019.02.029.

References

[1] J.F. Sallis, L.D. Frank, B.E. Saelens, M.K. Kraft, Active transportation and physical activity: opportunities for collaboration on transportation and public health research, Transp. Res. Part A Policy Pract. 38 (2004) 249–268 https://doi.org/10.1016/j.tra.2003.11.003.

[2] Seoul Metropolitan Subway Transportation Statistics, Information Plan Planner Statatistic Data Officer vol. 1, (2016) http://data.seoul.go.kr/dataList/datasetView.do?serviceKind=2&infId=273&srvType=S&stcSrl=273 , Accessed date: 1 February 2012.

[3] M. Kim, R.D. Braatz, J.T. Kim, C. Yoo, Indoor air quality control for improving passenger health in subway platforms using an outdoor air quality dependent ventilation system, Build. Environ. 92 (2015) 407–417 https://doi.org/10.1016/j.buildenv.2015.05.010.

[4] M. Kim, B. SankaraRao, O. Kang, J. Kim, C. Yoo, Monitoring and prediction of indoor air quality (IAQ) in subway or metro systems using season dependent models, Energy Build. 46 (2012) 48–55 https://doi.org/10.1016/j.enbuild.2011.10.047.

[5] E. V Bräuner, M. Frederiksen, B. Kolarik, L. Gunnarsen, Typical benign indoor aerosol concentrations in public spaces and designing biosensors for pathogen detection, Rev. Build. Environ. 82 (2014) 190–202 https://doi.org/10.1016/j.buildenv.2014.08.020.

[6] D.U. Park, K.C. Ha, Characteristics of PM10, PM2.5, CO2 and CO monitored in interiors and platforms of subway train in Seoul, Korea, Environ. Int. 34 (2008) 629–634 https://doi.org/10.1016/j.envint.2007.12.007.

[7] H. Liu, M. Kim, O. Kang, B. Sankararao, J. Kim, J.-C. Kim, C.K. Yoo, Sensor Validation for Monitoring Indoor Air Quality in a Subway Station, Indoor Built Environ. 21 (2012) 205–221, https://doi.org/10.1177/1420326x11419342.

[8] J. Loy-Benitez, P. Vilela, Q. Li, C.K. Yoo, Sequential prediction of quantitative health risk assessment for the fine particulate matter in an underground facility using deep recurrent neural networks, Ecotoxicol. Environ. Saf. 169 (2019) 316–324, https://doi.org/10.1016/j.ecoenv.2018.11.024.

[9] H. Liu, C. Yang, M. Huang, D. Wang, C.K. Yoo, Modeling of subway indoor air quality using Gaussian process regression, J. Hazard Mater. 359 (2018) 266–273, https://doi.org/10.1016/j.jhazmat.2018.07.034.

[10] H. Liu, C. Yang, M. Kim, C. Yoo, Fault Diagnosis of Subway Indoor Air Quality Based on Local Fisher Discriminant Analysis, Environ. Eng. Sci. 35 (2018) 0454, https://doi.org/10.1089/ees.2017.0454 ees.2017.

[11] D. Loomis, Y. Grosse, B. Lauby-Secretan, F. El Ghissassi, V. Bouvard, L. Benbrahim-Tallaa, N. Guha, R. Baan, H. Mattock, K. Straif, The carcinogenicity of outdoor air pollution, Lancet Oncol. 14 (2013) 1262–1263 https://doi.org/10.1016/S1470-2045(13)70487-X.

[12] I. Kloog, B. Ridgway, P. Koutrakis, B.A. Coull, J.D. Schwartz, Long- and short-term exposure to PM2.5 and mortality: using novel exposure models, Epidemiology 24 (2013) 555–561, https://doi.org/10.1097/EDE.0b013e318294beaa.

[13] L. Megido, B. Suárez-Peña, L. Negral, L. Castrillón, S. Suárez, Y. Fernández-Nava, E. Marañón, Relationship between physico-chemical characteristics and potential toxicity of PM10, Chemosphere 162 (2016) 73–79 https://doi.org/10.1016/j.chemosphere.2016.07.067.

[14] C. Colombi, S. Angius, V. Gianelle, M. Lazzarini, Particulate matter concentrations, Physical characteristics and elemental composition in the Milan underground transport system, Atmos. Environ. 70 (2013) 166–178, https://doi.org/10.1016/j.atmosenv.2013.01.035.

[15] Y.H. Cheng, Y.L. Lin, C.C. Liu, Levels of PM10 and PM2.5 in Taipei Rapid Transit System, Atmos. Environ. 42 (2008) 7242–7249, https://doi.org/10.1016/j.atmosenv.2008.07.011.

[16] K.Y. Kim, Y.S. Kim, Y.M. Roh, C.M. Lee, C.N. Kim, Spatial distribution of particulate matter (PM10 and PM2.5) in Seoul Metropolitan Subway stations, J. Hazard Mater. 154 (2008) 440–443, https://doi.org/10.1016/j.jhazmat.2007.10.042.

[17] M.J.R. Vilcassim, G.D. Thurston, R.E. Peltier, T. Gordon, Black carbon and particulate matter (PM2. 5) concentrations in New York City's subway stations, Environ. Sci. Technol. 48 (2014) 14738–14745.

[18] L. Guo, Y. Hu, Q. Hu, J. Lin, C. Li, J. Chen, L. Li, H. Fu, Characteristics and chemical compositions of particulate matter collected at the selected metro stations of Shanghai, China, Sci. Total Environ. 496 (2014) 443–452.

[19] V. Martins, T. Moreno, M.C. Minguillón, F. Amato, E. de Miguel, M. Capdevila, X. Querol, Exposure to airborne particulate matter in the subway system, Sci. Total Environ. 511 (2015) 711–722 https://doi.org/10.1016/j.scitotenv.2014.12.013.

[20] D. Park, M. Oh, Y. Yoon, E. Park, K. Lee, Source identification of PM10 pollution in subway passenger cabins using positive matrix factorization, Atmos. Environ. 49 (2012) 180–185 https://doi.org/10.1016/j.atmosenv.2011.11.064.

[21] T.J. Lee, J.S. Jeon, S.D. Kim, D.S. Kim, A comparative study on PM 10 source contributions in a Seoul metropolitan subway station before/after installing platform screen doors, J. Kor. Soc. Atmos. Environ. 26 (2010) 543–553.

[22] H.J. Jung, B. Kim, J. Ryu, S. Maskey, J.C. Kim, J. Sohn, C.U. Ro, Source identification of particulate matter collected at underground subway stations in Seoul, Korea using quantitative single-particle analysis, Atmos. Environ. 44 (2010) 2287–2293 https://doi.org/10.1016/j.atmosenv.2010.04.003.

[23] H. Maula, V. Hongisto, V. Naatula, A. Haapakangas, H. Koskela, The effect of low ventilation rate with elevated bioeffluent concentration on work performance, perceived indoor air quality, and health symptoms, Indoor Air 27 (2017) 1141–1153, https://doi.org/10.1111/ina.12387.

[24] L. Stabile, M. Dell'Isola, A. Frattolillo, A. Massimo, A. Russi, Effect of natural ventilation and manual airing on indoor air quality in naturally ventilated Italian classrooms, Build. Environ. 98 (2016) 180–189 https://doi.org/10.1016/j.buildenv.2016.01.009.

[25] T. Moreno, N. Pérez, C. Reche, V. Martins, E. de Miguel, M. Capdevila, S. Centelles, M.C. Minguillón, F. Amato, A. Alastuey, X. Querol, W. Gibbons, Subway platform air quality: Assessing the influences of tunnel ventilation, train piston effect and station design, Atmos. Environ. 92 (2014) 461–468 https://doi.org/10.1016/j.atmosenv.2014.04.043.

[26] Y.S. Son, T.V. Dinh, S.G. Chung, J. Lee, J.C. Kim, Removal of Particulate Matter Emitted from a Subway Tunnel Using Magnetic Filters, Environ. Sci. Technol. 48 (2014) 2870–2876, https://doi.org/10.1021/es404502x.

[27] M.J. Kim, R.D. Braatz, J.T. Kim, C.K. Yoo, Economical control of indoor air quality in underground metro station using an iterative dynamic programming-based ventilation system, Indoor Built Environ. 25 (2016) 949–961, https://doi.org/10.1177/1420326x15591640.

[28] H. Liu, S. Lee, M. Kim, H. Shi, J.T. Kim, K.L. Wasewar, C. Yoo, Multi-objective optimization of indoor air quality control and energy consumption minimization in a subway ventilation system, Energy Build. 66 (2013) 553–561, https://doi.org/10.1016/j.enbuild.2013.07.066.

[29] S. Lee, S. Hwangbo, J.T. Kim, C.K. Yoo, Gain scheduling based ventilation control with varying periodic indoor air quality (IAQ) dynamics for healthy IAQ and energy savings, Energy Build. 153 (2017) 275–286, https://doi.org/10.1016/j.enbuild.2017.08.021.

[30] D.E. Seborg, D.A. Mellichamp, T.F. Edgar, F.J. Doyle III, Process dynamics and control, John Wiley & Sons, 2010.

[31] P. Gopal, H. Chris, The Real-Time Optimisation of an Industrial Fermentation Process, IFAC Proc 37 (2004) 529–534 https://doi.org/10.1016/S1474-6670(17)32636-8.

[32] R.J. Wai, J.D. Lee, K.L. Chuang, Real-time PID control strategy for maglev transportation system via particle swarm optimization, IEEE Trans. Ind. Electron. 58 (2011) 629–646, https://doi.org/10.1109/TIE.2010.2046004.

[33] K. Englehart, B. Hudgins, A Robust, Real-Time Control Scheme for Multifunction Myoelectric Control, IEEE Trans. Biomed. Eng. 50 (2003) 848–854, https://doi.org/10.1109/TBME.2003.813539.

[34] W. Shengwei, J.T. Kim, S. Zhongwei, S. Yongjun, Z. Na, Online Optimal Ventilation Control of Building Air-conditioning Systems, Indoor Built Environ. 20 (2010) 129–136, https://doi.org/10.1177/1420326x10394491.

[35] S. Wang, D. Gao, Y. Sun, F. Xiao, An online adaptive optimal control strategy for complex building chilled water systems involving intermediate heat exchangers, Appl. Therm. Eng. 50 (2013) 614–628 https://doi.org/10.1016/j.applthermaleng.2012.06.010.

[36] S. Lee, H. Liu, M. Kim, J.T. Kim, C. Yoo, Online monitoring and interpretation of periodic diurnal and seasonal variations of indoor air pollutants in a subway station using parallel factor analysis (PARAFAC), Energy Build. 68 (2014) 87–98 https://doi.org/10.1016/j.enbuild.2013.09.022.

[37] K. OnYu, L. Hongbin, K. MinJeong, K. Jeong Tai, L.W. Kailas, Y. ChangKyoo, Periodic Local Multi-way Analysis and Monitoring of Indoor Air Quality in a Subway System Considering the Weekly Effect, Indoor Built Environ. 22 (2012) 77–93, https://doi.org/10.1177/1420326X12470285.

[38] S.W. Sung, J. Lee, I.B. Lee, Process identification and PID control, John Wiley & Sons, 2009.

[39] Y. Lu, S. Wang, Y. Zhao, C. Yan, Renewable energy system optimization of low/zero energy buildings using single-objective and multi-objective optimization methods,

Energy Build. 89 (2015) 61–75 https://doi.org/10.1016/j.enbuild.2014.12.032.
[40] KECO, What's CAI, Air Korea, 2013, https://www.airkorea.or.kr/eng/cai/cai1.
[41] T.S. Oh, M.J. Kim, J.J. Lim, O.Y. Kang, K. Vidya Shetty, B. SankaraRao, C.K. Yoo, J.H. Park, J.T. Kim, A real-time monitoring and assessment method for calculation of total amounts of indoor air pollutants emitted in subway stations, J. Air Waste Manag. Assoc. 62 (2012) 517–526, https://doi.org/10.1080/10962247.2012.660558.
[42] M. Brander, A. Sood, C. Wylie, A. Haughton, J. Lovell, Technical Paper| Electricity-specific emission factors for grid electricity, Ecometrica, Emiss. Com 37 (3) (2011).